Scientia Pharmaceutica

ÖSTERREICHISCHE PHARMAZEUTISCHE GESELLSCHAFT

MDPI

Article

Stability Enhancement and Skin Permeation Application of Nicotine by Forming Inclusion Complex with β-Cyclodextrin and Methyl-β-Cyclodextrin

Sorrawee Chulurks, Kulpavee Jitapunkul, Sasimas Katanyutanon, Pisanu Toochinda * and Luckhana Lawtrakul *

School of Bio-Chemical Engineering and Technology (BCET), Sirindhorn International Institute of Technology (SIIT), Thammasat University, Pathum Thani 12120, Thailand; sorrawee.chulurks@gmail.com (S.C.); kulpavee.work@gmail.com (K.J.); por.katanyutanon@gmail.com (S.K.)

* Correspondence: pisanu@siit.tu.ac.th (P.T.); luckhana@siit.tu.ac.th (L.L.)

Abstract: Nicotine is widely used in pharmaceutical industries, especially for smoking cessation in the form of transdermal patches. Nicotine gel in the patches has limitations from nicotine instability and high volatility. Thus, a nicotine preservation technique is needed. In this study, a nicotine encapsulation process using methyl-β-cyclodextrin (MβCD) is investigated and compared with β-cyclodextrin (βCD) to evaluate the preservation and skin permeation of nicotine. The M06-2X/6-31G(d,p) density functional theory calculations indicate a 1:1 host–guest molar ratio for the inclusion complex of nicotine with βCD and MβCD, which have been validated by experimental studies. The encapsulation efficiencies of βCD and MβCD to encapsulate nicotine are 59.96% and 63.76%, respectively. The preservation study of the inclusion complexes compared to pure nicotine shows a stability improvement of nicotine after being encapsulated. After 21 days, the percentages of the nicotine/βCD and nicotine/MβCD inclusion complexes that remain are 89.32% and 76.22%, while only 65.56% of pure nicotine remains. Besides the one-hour skin permeation tests, the amounts of nicotine permeated through pig skin from the nicotine/βCD and nicotine/MβCD inclusion complex gels are 14 and 10 times as much as the pure nicotine gel, respectively. Therefore, the encapsulation of nicotine with βCD and MβCD can be used to enhance the stability and skin permeation application of nicotine-containing products.

Keywords: cyclodextrin; encapsulation; molecular modeling; nicotine; preservation; skin permeation

Citation: Chulurks, S.; Jitapunkul, K.; Katanyutanon, S.; Toochinda, P.; Lawtrakul, L. Stability Enhancement and Skin Permeation Application of Nicotine by Forming Inclusion Complex with β-Cyclodextrin and Methyl-β-Cyclodextrin. *Sci. Pharm.* **2021**, *89*, 43. https://doi.org/10.3390/scipharm89040043

Academic Editor: Roman B. Lesyk

Received: 7 September 2021
Accepted: 24 September 2021
Published: 28 September 2021

1. Introduction

Nicotine, an alkaloid compound composed of pyrrolidine and pyridine rings, is found in tobacco leaves [1–3]. In the pharmaceutical industry, nicotine is widely used for nicotine replacement therapy and for recovering patient health conditions from dementia, schizophrenia, dopaminergic neuron, and axon dysfunction [4]. Some research shows the use of nicotine in reducing the symptoms of Parkinson's and Alzheimer's diseases [5–7]. A major nicotine delivery method used in these therapies is a transdermal patch. The shelf life of transdermal patches is largely affected by the high volatility and hygroscopic property of nicotine [8]. Therefore, the preservation or the improvement of nicotine stability is needed to improve its shelf life. A preservation method that is mainly used in the food and pharmaceutical industries is the encapsulation technique [9–12].

Encapsulations can be defined as host–guest complexes that are composed of two or more molecules that are held together by intermolecular forces compared to bonding. This technique is employed to enhance the protection of bioactive compounds (the guests) against degradation. β-cyclodextrin (βCD) is the most common host molecule for the encapsulation of active compounds from plants due to its cost-effectiveness and high possibility of forming inclusion complexes [9,10]. Moreover, the Food and Drug

Administration (FDA) approved βCD as a nontoxic substance to be used in food and pharmaceutical applications [11,12]. There are several studies that have reported that nicotine can form an inclusion complex with βCD [8,13]. However, the low aqueous solubility of βCD (18.5 mg/mL) may limit the inclusion complex formation. To improve the inclusion complex formation, methyl-β-cyclodextrin (MβCD), a derivative of βCD was introduced as an alternative host molecule due to its higher aqueous solubility (>500 mg/mL). Since there is no report about the inclusion complex formation between nicotine and MβCD, a computational simulation was performed to investigate the inclusion complex formation possibility between nicotine and MβCD prior to the laboratory test.

Nicotine was introduced as a guest molecule, while CDs (βCD and MβCD) were introduced as host molecules. The host–guest ratio suggestion obtained from the computer simulation was implemented in the experimental study for inclusion complex preparation. Since ethanol is another common cosolvent for the inclusion complex preparation process, the effect of the ethanol concentration in the preparation process was also studied. For solid complex recovery, a solvent evaporation method by oven drying was chosen due to its easy operation and low cost [14]. The preservation of nicotine in the form of inclusion complexes was evaluated and compared to pure nicotine in different storage temperatures after 21 days. Since nicotine in the pharmaceutical industry is used in the form of a transdermal patch, the release of encapsulated nicotine through the skin must also be investigated. In the lab, Franz's diffusion cell was used to evaluate the permeability of a pure nicotine gel and nicotine in the form of inclusion complexes through pig skin.

Therefore, this study was focused on: (1) the determination of an inclusion complex formation possibility and the host–guest molar ratio between nicotine and CDs by computational simulation, (2) determination of the encapsulation efficiency of the nicotine/CDs inclusion complex in the laboratory, (3) evaluation of the preservation efficiency of the nicotine/CDs inclusion complex, and (4) investigation of the skin permeation of nicotine in the form of inclusion complexes compared to nicotine in a free form.

2. Materials and Methods

2.1. Materials

(S)-Nicotine (99%, Alfa Aesar, Haverhill, MA, USA) was used as the guest molecule for nanoencapsulation and the standard for the calibration curve. βCD (98.0%, Tokyo Chemical Industry, Tokyo, Japan) and MβCD (a mixture of several methylated, Tokyo Chemical Industry, Tokyo, Japan) with the moles of the methyl substitution group of 1.6–1.9 per glucose unit were used as host molecules for nicotine. For nicotine/CDs inclusion complex characterization, absolute ethanol (HPLC grade, RCI Labscan, Bangkok, Thailand) was used as a solvent to prepare the nicotine standard solution for GC-FID and to extract nicotine from the inclusion complex. Nicotine gels were prepared for the skin permeation study. Carbopol gel was prepared by using carbopol 940 dissolved with ethanol (AR grade, RCI Labscan, Bangkok, Thailand) and propylene glycol (Laboratory reagent, KEMAUS, Sydney, NSW, Australia). Phosphate buffer solution, methanol (AR grade, RCI Labscan, Bangkok, Thailand), and triethylamine (Laboratory reagent, KEMAUS, Sydney, NSW, Australia) were used as the mobile phases to determine the amount of permeated nicotine through pig skin by HPLC.

2.2. Computational Simulation of Nicotine/CDs Inclusion Complex

A computational simulation was performed to determine the forming possibility of an inclusion complex between nicotine and CDs (βCD and MβCD), as well as the conformations. The X-ray crystal structures of nicotine, βCD, and MβCD were downloaded from the Cambridge Crystallographic Data Centre with identifiers: YOCZUM [15], BCDEXD03 [16], and BOYFOK03 [17], respectively (Figure 1). The downloaded structure of 2,6-O-methyl-β-cyclodextrin is crystalline MβCD. On the other hand, MβCD used in the experiment was the randomly methylated βCD, which is amorphous MβCD without a specific crystalline structure. However, crystalline MβCD should be able to demonstrate the possibility of an

inclusion complex forming due to similarity in the molecular structure with the amorphous derivatives. The modification of the atoms and bonds in all structures was done using Discovery Studio 4.0 Visualizer (BIOVIA, San Diego, CA, USA) [18]; then, the geometry optimization was perform in the Gaussian16 program package (Gaussian, Inc., Wallingford, CT, USA) [19] using density functional theory (DFT) M06-2X with the 6-31G(d,p) basis set. The optimized nicotine was then docked into the cavity of both βCD and MβCD molecules via AutoDock 4.2 [20]. The βCD and MβCD molecules (hosts) were kept rigid, while the nicotine molecule (guest) was allowed to move freely inside the host's cavity. One hundred docking calculations were performed on each host–guest complex using the Lamarckian genetic algorithm with the remaining parameters run at default settings [20]. The results obtained were classified into different clusters with different molecular docking binding energies. The docked conformation with the lowest energy in each cluster was selected to be the representative for further minimization using the M06-2X/6-31G(d,p) method. The complexation energy (ΔE) of the 1:1 molecular ratio between nicotine/βCD and nicotine/MβCD in the minimized geometries was evaluated by Equation (1):

$$\Delta E = E_{\text{complex}} - (E_{\text{host}} + E_{\text{guest}}) \quad (1)$$

where E_{complex}, E_{host}, and E_{guest} represent the minimization energy of the host/guest inclusion complex, the host molecule (either βCD or MβCD), and the guest molecule (nicotine), respectively.

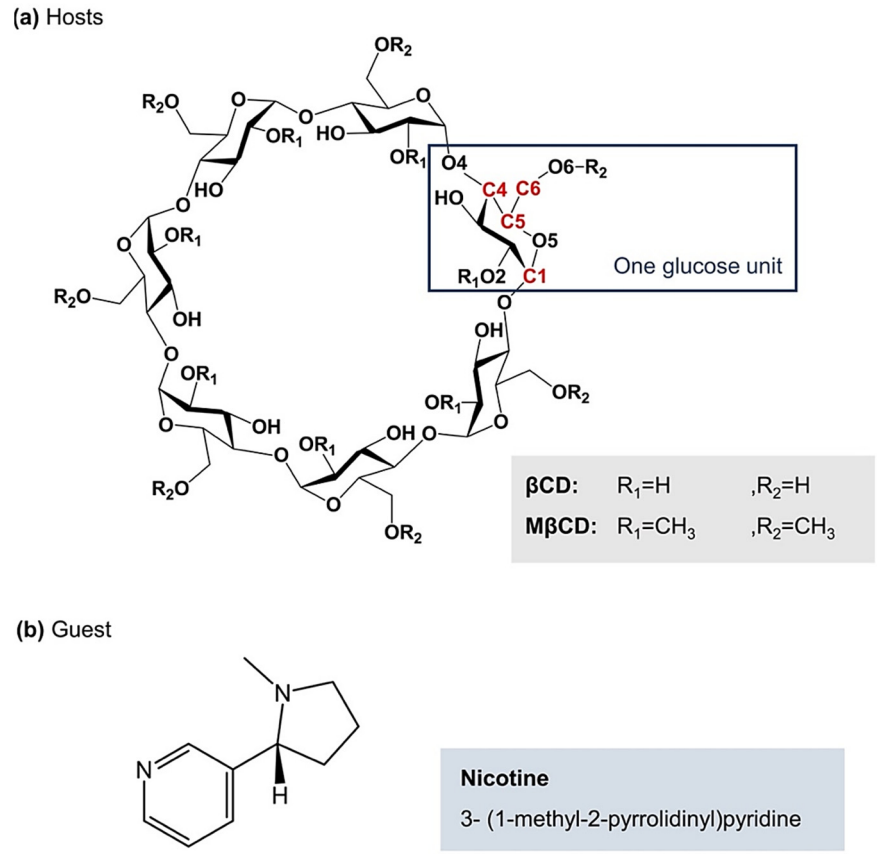

Figure 1. Schematic representation of (**a**) the glucose unit and atomic numbering of βCD and MβCD and (**b**) nicotine structure (C1, C4, C5, and C6 are the carbon atom positions with numeric indexes in each glucose unit).

2.3. Determination of the Host–Guest Molar Ratio of Nicotine/CDs Inclusion Complex by Job's Method

The host–guest ratio of the nicotine/CDs inclusion complex was determined by the continuous variation method (Job's method). The changes in the absorbance of nicotine/CDs inclusion complex solutions prepared with different host–guest molar ratios were investigated. Nicotine, βCD, and MβCD were prepared separately in deionized water and mixed together at different host–guest molar ratios to obtain solutions with the total concentration of 0.3 mM. The absorbance of nicotine was recorded at 260 nm and 25 °C, as mentioned in the HPLC condition by the UV/Visible spectrometer (Genesys 10s, Thermo Fisher Scientific, Waltham, MA, USA). Job's plot was prepared by plotting the product of the host–guest molar ratio and the changes in absorbance at each host–guest molar ratio.

2.4. Nicotine/CDs Inclusion Complex Preparation Method

Appropriate amounts of MβCD and βCD were dissolved in 30 mL of water to create 16-mM solutions. Nicotine was added at a 1:1 host–guest molar ratio to each the CD solution as the results from the computer simulation suggested. The solutions were mixed in an incubator shaker at 25 °C for 72 h. Solid complexes were recovered by the oven-drying method at 60 °C for 72 h and stored at 4 °C. To confirm the inclusion complex formation, physical mixtures (PM), the mixing between pure nicotine and CDs by the kneading method with the same ratio of inclusion complex preparation, were introduced as the representative of unbonded nicotine and CDs to compare with pure CDs and inclusion complexes in the characterization methods.

2.5. Solvent Effect on the Encapsulation Efficiency of Nicotine/CDs Inclusion Complex

Ethanol is generally used as a cosolvent for the inclusion complex preparation process to improve the encapsulation efficiency [21]. Hence, the effect of various concentrations of ethanol on the encapsulation efficiency of CDs was investigated. βCD and MβCD were dissolved in 10 mL of 0, 5, and 10 vol% of ethanol–water solutions to create 16 mM of CD solutions. After being fully dissolved, nicotine was added at a 1:1 host–guest molar ratio into each solution, and the solutions were mixed in an incubator shaker at 25 °C for 72 h for the inclusion complex formation. The solid complexes were recovered from the inclusion complex solutions by the oven-drying method and stored at 4 °C.

Nicotine encapsulated in the solid complexes was extracted in pure ethanol with the ratio of 10-mg solid per 1-mL solvent and quantified by GC-FID. Since βCD has a low aqueous solubility, the extraction of nicotine from the nicotine/βCD solid complex required sonication, which was performed at 40 °C for 45 min. The encapsulation efficiency was determined using Equation (2):

$$\%\text{Encapsulation eff.} = \frac{\text{Amount of encapsulated nicotine}}{\text{Amount of nicotine initially added}} \times 100 \quad (2)$$

2.6. Nicotine/CDs Inclusion Complex Characterization

2.6.1. Gas Chromatography Coupled with Flame Ionization Detector (GC-FID)

The encapsulation efficiency of the nicotine/CDs inclusion complex was determined by GC-FID (Clarus 580, Perkin Elmer, Waltham, MA, USA) coupled with an HP-5 ((5%-phenyl)-methylpolysiloxane, 30-m length × 0.25-mm I.D. × 0.25-μm film column, Agilent, Santa Clara, CA, USA). One microliter of injection volume was set with a split ratio of 10:1. The injection temperature was 260 °C. Helium was used as a carrier gas with the flow rate of 2 mL/min. The temperature program was set at 120 °C and held for 2 min. Then, the temperature was ramped up to 250 °C at a rate of 15 °C/min and held for 2 min. The detector temperature was set at 260 °C, and the range of detector was 1 with an attenuation of 5. All the GC samples were filtered by a 0.22-μm syringe filter before injection.

2.6.2. Thermogravimetric Analysis (TGA)

The thermal analysis of the nicotine/CDs inclusion complex, physical mixtures, and pure compounds were analyzed by TGA/DSC 1 (Mettler-Toledo, Columbus, OH, USA). The TG and DTG curves of the samples were recorded. The samples were weighed and placed in alumina crucibles. The samples were heated from 30 °C to 500 °C at 10 °C/min under N_2 atmosphere with a 50-mL/min flow rate.

2.6.3. Differential Scanning Calorimetry (DSC)

The energy changes of the nicotine/CDs inclusion complex, physical mixtures, and pure compounds with increasing temperatures were analyzed by DSC 3+ (Mettler-Toledo, Columbus, OH, USA). The samples were weighed, placed in aluminum crucibles, and heated from 30 °C to 300 °C at the rate of 10 °C/min under N_2 atmosphere with a 50-mL/min flow rate.

2.6.4. X-ray Diffractometry (XRD)

The crystalline patterns of the CDs, nicotine/βCD inclusion complex, and nicotine/MβCD inclusion complex were characterized to confirm the inclusion complex formation between the nicotine and CDs by XRD (D8 Advance Model, Bruker, Coventry, UK) to investigate the inclusion complex formation. XRD was operated at a voltage of 40 kV and a current of 45 mA and a temperature of 25 °C. The crystalline patterns were recorded between 3° and 40° (2θ) with a 0.02° step size and 0.5-s step time. Pure nicotine is in liquid form, which cannot be characterized by XRD. Therefore, physical mixtures between pure nicotine and CDs prepared by the kneading method were introduced as the representative of unbonded nicotine and CDs to compare with pure CDs and inclusion complexes.

2.6.5. Fourier-Transform Infrared Spectroscopy (FTIR)

A FTIR spectrometer (Nicolet iS50, Thermo Fisher Scientific, Waltham, MA, USA) was used to observe the functional groups of the βCD, MβCD, nicotine, and inclusion complexes to confirm the inclusion complex formation. The analyzed samples were prepared by mixing 1% (*w*/*w*) of solid complexes with spectral grade KBr (Specac, Washington, PA, USA) and ground into powder. The pure liquid nicotine was characterized using the attenuated total reflection (ATR) mode. The spectrogram of each sample was recorded at wavenumbers between 400 cm^{-1} and 4000 cm^{-1} with 16 scans and a resolution of 4 cm^{-1}.

2.6.6. High-Performance Liquid Chromatography (HPLC)

The amount of permeated nicotine through pig skin was determined by a 1260 Infinity II LC system (Agilent Technologies, Santa Clara, CA, USA) equipped with a quaternary pump (Model: G7111A), a vial sampler (Model: G7129A), a multicolumn thermostat (Model: G7116A), and a variable wavelength detector (Model: G7114A). The separation was performed on a Luna 5-µm C18(2) 100 Å, 250-mm × 4.6-mm column (Phenomenex, Santa Clara, CA, USA), which was controlled at 25 °C. The mobile phase was a mixture of a 0.08-M phosphate buffer with pH 6.5, methanol, and triethylamine with a volume ratio of 55.8:40:4.2 with a flow rate of 1 mL/min. The injection volume was 20 µL, and the wavelength of the detector was set at 260 nm.

2.7. Preservation Study of the Nicotine/CDs Inclusion Complex

The evaluation of nicotine preservation after being encapsulated in the form of inclusion complexes compared to pure nicotine was performed at the storage temperatures of 25 °C and 40 °C with a duration of 21 days. Nicotine/βCD, nicotine/MβCD inclusion complexes, and pure nicotine with 15 mg of nicotine content were separately stored in an incubator. The evaluation was performed in triplicate. The remaining nicotine after air exposure at different temperatures and periods of time was extracted by ethanol and quantified by GC-FID. The amount of nicotine encapsulated by CDs before the preserva-

tion study (day 0) was counted as 100%. The percentage of the remaining nicotine was determined by Equation (3):

$$\%\text{Remaining nicotine} = \frac{\text{Amount of nicotine remained}}{\text{Amount of nicotine encapsulated}} \times 100 \quad (3)$$

2.8. Skin Permeation Study of the Nicotine/CDs Inclusion Complex

The permeation rate of nicotine in the form of inclusion complexes compared to pure nicotine was studied in Franz's diffusion cell (Logan Instrumental Corp., Model FDC-6, Somerset, NJ, USA). Each of the inclusion complexes was distributed in carbopol gel and placed in contact with the medium surface for the permeation rate evaluation. The gel was prepared by mixing 1% (*w*/*w*) of carbopol 940 powder in an ethanol–water solution (120 g of water with 100 g of ethanol) and stirring at 900 rpm for 10 min. The carbopol gel was left to swell for at least 10 h. One gram of each solid inclusion complex was added into 2.5 mL of water and mixed with 25 g of the prepared carbopol gel. A small amount (0.89 mL) of propylene glycol was added to serve as a solubilizer. Lastly, the well-mixed nicotine gel was left overnight.

For Franz's diffusion cell preparation, the newborn pig skin was used as the medium to evaluate the nicotine skin permeability due to its significant similarity to human skin [20]. Francesco Cilurzo, Paola Minghetti, and Chiara Sinico studied the preparation of pig skin as a membrane for drug permeation [22]. In this study, the pig skin was prepared following the procedure outlined in Cilurzo's study. Subcutaneous fat was removed from the pig skin before it was cut into 3 × 3-cm^2 pieces and stored at −18 °C. The storage temperature was changed to 4 °C one day before performing the experiment. The pig skin was mounted between the two half-cells of Franz's diffusion cell with its dermis surface facing the receptor half-cell. The prepared nicotine gel was placed in contact with the pig skin surface. The receptor solution (isotonic saline pH 7.4) was added into the receptor half-cell and collected periodically to determine the concentration of permeated nicotine using HPLC.

3. Results

3.1. Computational Simulation of the Nicotine/CDs Inclusion Complex

Two possible modes of nicotine orientation inside the cavity of CDs are shown in Figure 2. In orientation A, the pyridine ring of nicotine is located near the wide rim of the host molecule, while, in orientation B, the pyrrolidine moiety of nicotine is located near the wide rim of the host molecule. The complexation energy and the optimized inclusion complex conformations obtained from the M06-2X/6-31G(d,p) calculations are presented in Table 1 and Figure 3, respectively.

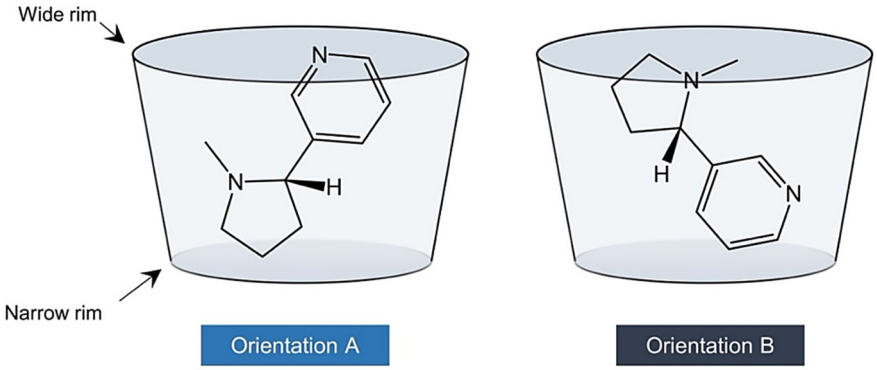

Figure 2. Schematic illustration of two possible conformations of the nicotine/CDs inclusion complex.

Table 1. The calculated complexation energy (Δ*E*), in kcal/mol, of the nicotine inclusion complex with βCD and MβCD.

	Orientation A	Orientation B
Nicotine/βCD	−24.51	−26.13
Nicotine/MβCD	−17.41	−22.73

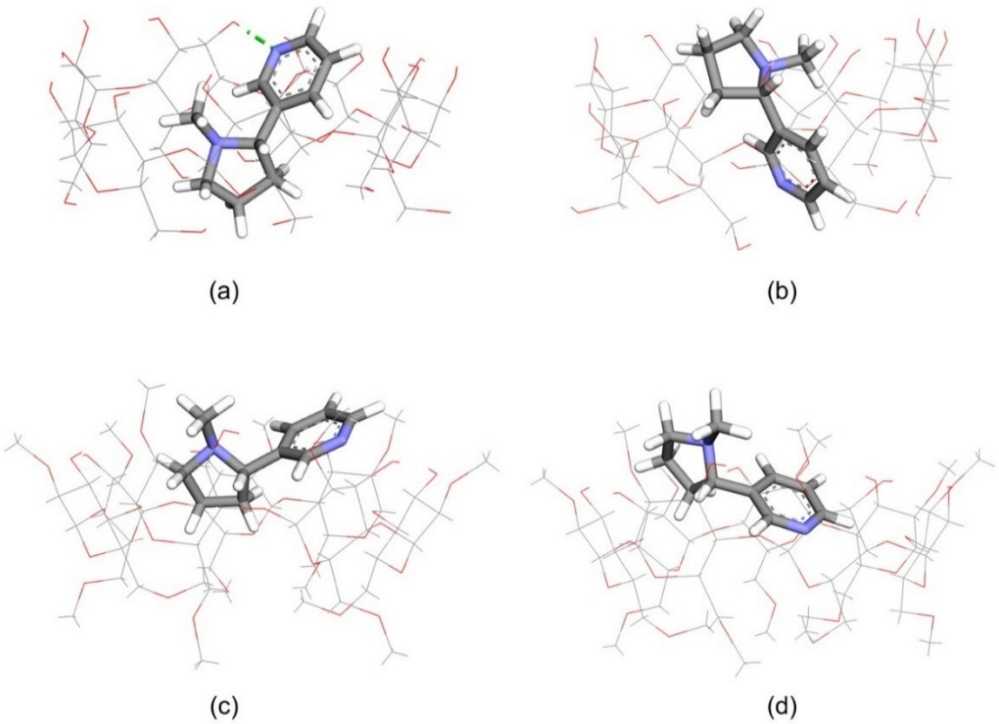

Figure 3. The minimized inclusion complex conformations: (**a**) nicotine/βCD in orientation A, (**b**) nicotine/βCD in orientation B, (**c**) nicotine/MβCD in orientation A, and (**d**) nicotine/MβCD in orientation B. βCD and MβCD are presented as a line model. The nicotine molecule is presented as a stick model. The green dashed line refers to a hydrogen bond.

All negative values of the complexation energy (Δ*E*) indicate that nicotine can form a stable 1:1 inclusion complex with βCD and MβCD in both orientation A and B. It has been shown that nicotine is trapped deep inside the cavity and forms a considerably stronger binding to βCD than MβCD in the same orientation, with a magnitude of 7.1 and 3.40 kcal/mol in orientation A and B, respectively (as shown in Figure 3 and Table 1). In nicotine/βCD orientation A, one H-bond with a distance of 2.08 Å occurs between a nitrogen atom of the pyridine ring and hydrogen atom of the secondary hydroxyl group at the C2 atom of βCD, as shown in Figure 3a. No intermolecular H-bond is found in nicotine/βCD orientation B and the nicotine/MβCD complexes in both orientations.

Some of the methyl tails attached to the O6 atom of MβCD entered and occupied the inner cavity, as depicted in Figure 3c,d. Consequently, the binding cavity of MβCD is shallower than βCD and prevents the entry of nicotine molecules, which results in the alignment of guest molecules near the wider rim of MβCD. Methyl substitution at the C2 atom for all seven glucose units increases the number of hydrocarbon atoms, which enhances the hydrophobic interaction between the host and the guest molecules, especially in orientation B (Figure 3d). Therefore, the computational results indicate a possibility of nicotine/MβCD inclusion complex formation with the same host–guest ratio as the nicotine/βCD inclusion complex. The theoretical study on inclusion complexes by computational simulation was used as the preliminary results to the experimental study in the laboratory scale.

3.2. Determination of the Host–Guest Molar Ratio of the Nicotine/CDs Inclusion Complex by Job's Method

To verify the host–guest ratios of the nicotine/βCD and nicotine/MβCD inclusion complexes obtained from the computational simulation, the continuous variation method (Job's plot) was performed. The absorbance (A) at 260 nm was recorded at different host–guest ratios (R). The total concentration of the nicotine/CD solutions was kept constant at 0.3 mM while varying the host–guest ratios of the nicotine and CDs from 0 to 1. The change in the absorbance (ΔA) was compared relative to when R = 1. Figure 4a,b shows the Job's plots of the nicotine/βCD and nicotine/MβCD inclusion complex systems, respectively, which show the maxima at R = 0.50. According to the method, the host–guest molar ratios of the complexes can be obtained by the value of R at the maxima curve, i.e., the host–guest molar ratio is 1:2, 1:1, and 2:1 when R is equal to 0.66, 0.50, and 0.33, respectively. Therefore, the host–guest molar ratio of both the nicotine/βCD and nicotine/MβCD inclusion complexes is at 1:1.

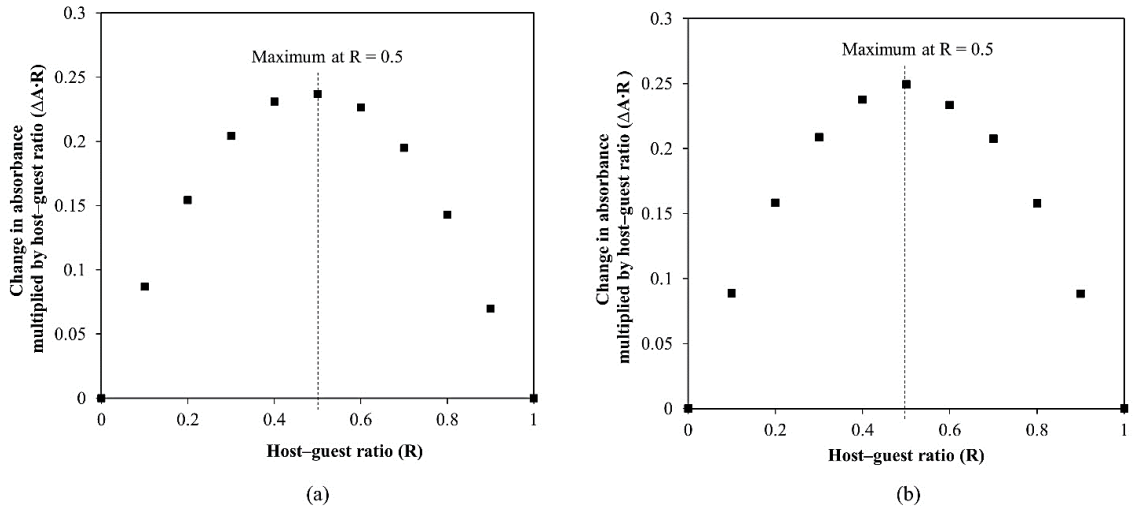

Figure 4. Continuous variation plot (Job's plot) of (**a**) the nicotine/βCD inclusion complex and (**b**) nicotine/MβCD inclusion complex.

3.3. Solvent Effect on the Encapsulation Efficiency of the Nicotine/CDs Inclusion Complex

The nicotine/CDs inclusion complex encapsulation efficiencies prepared in the different ethanol concentrations are shown in Table 2. The results demonstrated that increasing the ethanol concentration as a cosolvent in the inclusion complex preparation process decreased the encapsulation efficiencies. The highest encapsulation efficiencies of the nicotine/βCD inclusion complex and nicotine/MβCD inclusion complex were 59.96% and 63.76%, respectively, obtained without the addition of ethanol. Therefore, the presence of ethanol causes nicotine to stay in a free form in the ethanol solution rather than forming an inclusion complex. Thus, using pure water as the solvent is suitable for the inclusion complex preparation of nicotine and CDs.

Table 2. Encapsulation efficiency of CDs with varied ethanol contents used for inclusion complex preparation.

Inclusion Complex	Concentration of Ethanol (vol%)	Encapsulation Efficiency (%)
Nicotine/βCD	0	59.96 ± 1.62
	5	57.45 ± 1.06
	10	49.91 ± 1.26
Nicotine/MβCD	0	63.76 ± 0.24
	5	61.09 ± 1.25
	10	60.09 ± 1.26

3.4. Nicotine/CDs Inclusion Complex Characterization

3.4.1. Thermogravimetric Analysis (TGA)

Figure 5a–d shows the TG and DTG curves of the nicotine/CDs inclusion complex, pure βCD, MβCD, nicotine, and physical mixtures as references of unbonded nicotine and CDs. The TG and DTG profiles of βCD and MβCD show two-step weight losses from the loss of moisture content from 30 to 100 °C and their thermal decomposition at 320 °C, while the TG and DTG profiles of nicotine in the free form show a weight loss in the range between 25 °C and 230 °C from its volatilization. The TG and DTG profiles of the physical mixtures of both nicotine/βCD and nicotine/MβCD show the weight loss at the same temperature as in pure compounds. In contrast, the TG and DTG profiles of the nicotine/βCD and nicotine/MβCD inclusion complexes show the loss of the moisture content and thermal decomposition of the CDs without the volatilization of nicotine. Therefore, the improved thermostability of nicotine after encapsulation confirms the inclusion complex formation between nicotine and CDs.

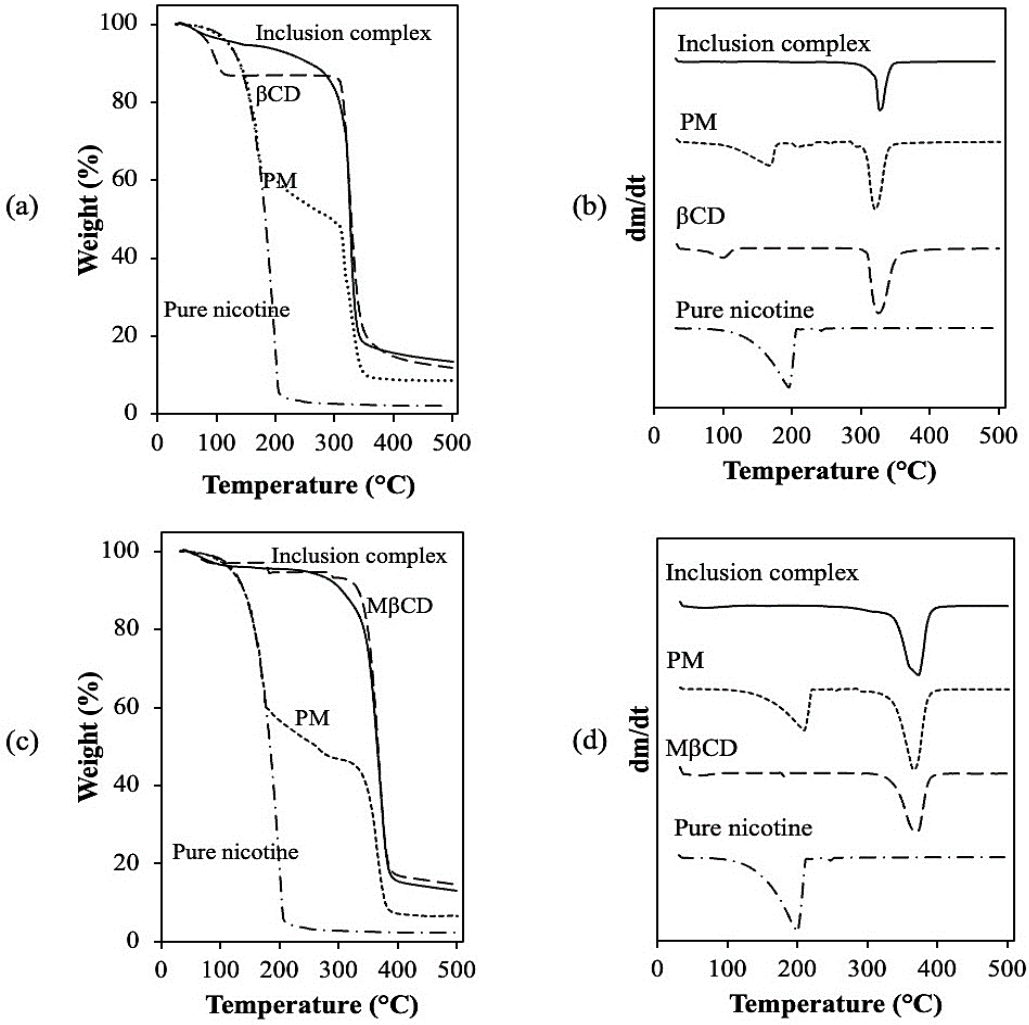

Figure 5. Thermal analysis curves of the inclusion complexes; (**a**) TG and (**b**) DTG curves of nicotine/βCD and (**c**) TG and (**d**) DTG curves of nicotine/MβCD.

3.4.2. Differential Scanning Calorimetry (DSC)

Figure 6 shows the DSC curves of the nicotine/CDs inclusion complex compared to the physical mixtures as references, pure βCD, MβCD, and nicotine. Pure nicotine provides two endothermic peaks. The first peak between 25 and 70 °C corresponds to the loss of moisture content due to its hygroscopic nature. The second peak, as shown in a

circle between 150 and 220 °C, corresponds to the volatilization of nicotine. For βCD and MβCD, the results showed a broad endothermic peak from 30 to 120 °C from the loss of the moisture content. DSC curves of the physical mixtures show the same endothermic peaks as pure CDs combined with the volatilization of nicotine. In contrast, for both the nicotine/βCD and nicotine/MβCD inclusion complexes, the results showed only a broad endothermic peak from 30 to 150 °C from the loss of the moisture content. Since there is no peak corresponding to the loss of nicotine from volatilization in the complex curves, the DSC results imply inclusion complex formation between nicotine and the CDs.

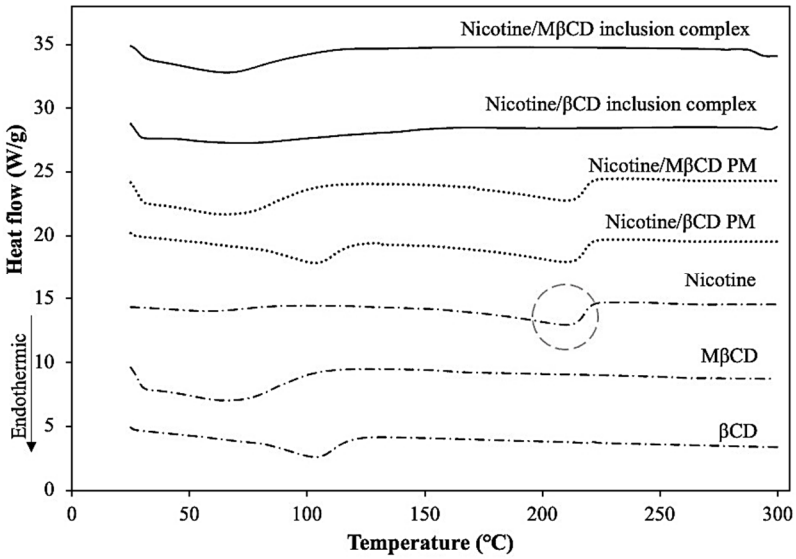

Figure 6. DSC curves of inclusion complexes nicotine/MβCD, nicotine/βCD, PMs, nicotine, MβCD, and βCD.

3.4.3. X-ray Diffractometry (XRD)

According to the liquid form of pure nicotine in this study, pure nicotine cannot be characterized by XRD. From the literature, a physical mixture (PM) between host and guest molecules can be used as a reference of unbonded host and guest for comparing the crystalline pattern with the inclusion complex to confirm inclusion complex formation [23,24]. Therefore, physical mixtures between pure nicotine and CDs prepared by the kneading method were introduced as the representative of unbonded nicotine and CDs to compare with pure CDs and inclusion complexes. Figure 7a illustrates the crystalline pattern of βCD, the physical mixture of nicotine and βCD, and the nicotine/βCD inclusion complex. The XRD pattern of the physical mixture is similar to the βCD pattern, while the nicotine/βCD inclusion complex shows a different pattern. This difference in the crystallinity of the nicotine/βCD inclusion complex confirms the inclusion complex formation. Figure 7b shows the crystalline pattern of MβCD. The lack of defined peaks in the XRD pattern confirms the amorphous structure of MβCD. Hence, due to the amorphous structure of MβCD, the XRD technique cannot be used to confirm the inclusion complex formation between nicotine and MβCD.

3.4.4. Fourier-Transform Infrared Spectroscopy (FTIR)

FTIR was used to confirm the inclusion complex formation between nicotine (guest) and the CDs (host). Figure 8 illustrates the IR spectra of the inclusion complexes, βCD, MβCD, and pure nicotine. To confirm the inclusion complex formation between nicotine and MβCD, the peak shifts of IR spectra of the nicotine/MβCD inclusion complex compared to the pure compounds were investigated with the analysis from the nicotine/βCD inclusion complex as a reference.

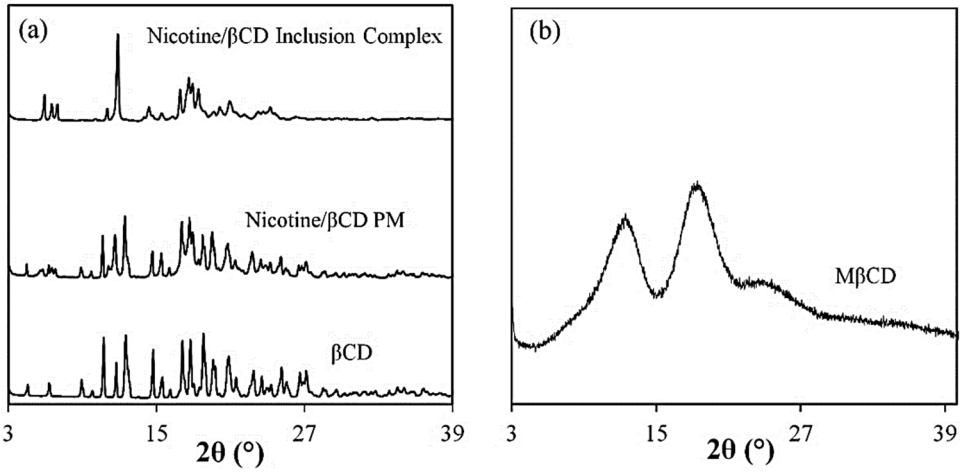

Figure 7. XRD patterns of (**a**) the nicotine/βCD inclusion complex, nicotine/βCD PM, and βCD and (**b**) pure MβCD.

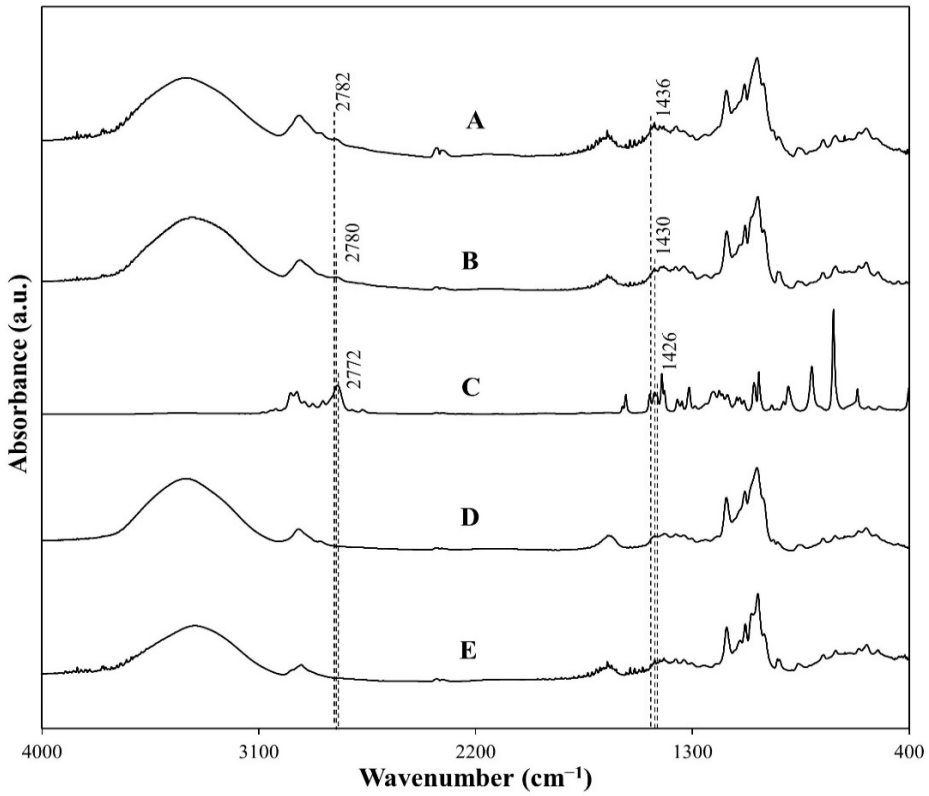

Figure 8. IR spectrum of (**A**) the nicotine/MβCD inclusion complex, (**B**) the nicotine/βCD inclusion complex, (**C**) nicotine, (**D**) MβCD, and (**E**) βCD.

According to Figure 8, the characteristic peaks of nicotine are observed at 2272 cm^{-1} and 1426 cm^{-1}, corresponding to N-CH_3 stretching and C-N stretching, respectively. The inclusion complex formation between nicotine and the CDs is indicated by the peak shifts, which are related to the interactions between nicotine and both CDs. The IR spectrum of the nicotine/βCD inclusion complex shows inclusion complex formation with two subtle peak shifts, which correspond to N-CH_3 stretching (2780 cm^{-1}) and C-N stretching (1430 cm^{-1}). The IR spectrum of the nicotine/MβCD inclusion complex also shows shifting in the same way as the IR spectrum of the nicotine/βCD inclusion complex, which corresponds to N-CH_3 stretching (2782 cm^{-1}) and C-N stretching (1436 cm^{-1}). Moreover, some peaks from nicotine become lower or almost disappear in all the inclusion complexes, which

might come from the encapsulation of nicotine inside CD cavities. As evident from the IR spectrum of both the nicotine/βCD and nicotine/MβCD inclusion complexes, nicotine can form inclusion complexes with βCD and MβCD. Therefore, all the characterization results confirm the inclusion complex formation between nicotine and both CDs.

3.5. Preservation Study of Nicotine/CDs Inclusion Complex

The preservation of nicotine in the inclusion complexes was evaluated at 25 °C and 40 °C with 95% humidity for 21 days and compared to pure nicotine, as shown in Figure 9a,b. At 25 °C, the remaining nicotine from pure nicotine after 21 days was 71.58%, while the remaining nicotine from the nicotine/βCD and nicotine/MβCD inclusion complexes was 85.84% and 82.72%, respectively, which was more than 1.2 times as much as pure nicotine. At 40 °C, the remaining nicotine from pure nicotine after 21 days was 65.56%, while the remaining nicotine from the nicotine/βCD and nicotine/MβCD inclusion complexes was 89.32% and 76.22%, respectively, which was more than 1.2 times as much as pure nicotine. The amount of remaining nicotine from the nicotine/MβCD inclusion complex is lower than from the nicotine/βCD inclusion complex. This agrees with our DFT calculations that nicotine forms considerably stronger binding to βCD than MβCD in the same orientation, which is indicated by its lower complexation energy (Δ*E*; Table 1).

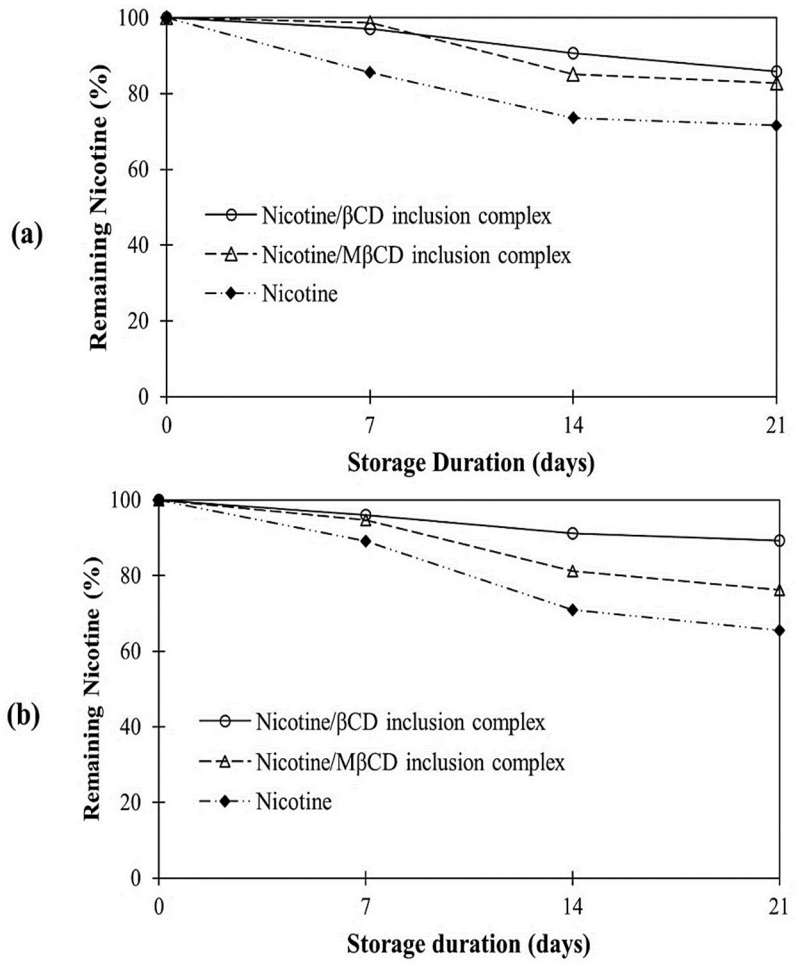

Figure 9. Preservation of nicotine in the form of a free compound and inclusion complexes (**a**) at 25 °C and (**b**) at 40 °C.

Since air at 25 °C has a lower vapor pressure (22.61 mmHg) than air at 40 °C (52.54 mmHg), the presence of water in the air at 25 °C is lower as well. Therefore, due to

the high aqueous solubility of MβCD, the cause of instability of the nicotine/MβCD inclusion complex at 40 °C may be the presence of water in the air, which leads to the dissolution of MβCD and a decreasing amount of nicotine. However, the encapsulation of nicotine by both βCD and MβCD increases the amount of the remaining nicotine. Therefore, βCD and MβCD can be used to preserve nicotine in the form of the inclusion complexes.

3.6. Skin Permeation Study of the Nicotine/CDs Inclusion Complexes

Table 3 shows the amount of permeated nicotine through pig skin using pure nicotine and inclusion complexes in the form of gels. The amounts of nicotine permeated through pig skin from nicotine/βCD and nicotine/MβCD are higher than that from pure nicotine. After 30 min, the amounts of nicotine permeated through pig skin from the nicotine/βCD and nicotine/MβCD inclusion complex gels are nine times as much as pure nicotine gel. After 60 min, the amounts of nicotine permeated through pig skin from the nicotine/βCD and nicotine/MβCD inclusion complex gels are 14 and 10 times as much as pure nicotine gel, respectively. The amount of permeated nicotine from the inclusion complex is higher, especially from the nicotine/βCD inclusion complex. Thus, the skin permeation study concludes that the permeability of nicotine depends on the nicotine stability, which relates to the amount of remaining nicotine in the gel after a period. The results from a nicotine permeation study can be used in the nicotine transdermal patch production process to optimize the production cost. Since the nicotine permeability is increased, the required amount of nicotine loading in the transdermal patch will be decreased. Therefore, the improvement in nicotine permeability after being encapsulated can be applied to develop nicotine transdermal patches that are more efficient.

Table 3. Amount of permeated nicotine from gel.

Sample Names	Amount of Nicotine (μg)	
	After 30 min	After 60 min
Nicotine/βCD gel	4.08 ± 0.63	13.57 ± 0.18
Nicotine/MβCD gel	3.82 ± 0.67	9.81 ± 0.11
Pure nicotine gel	0.42 ± 0.02	0.95 ± 0.03

4. Conclusions

The encapsulation of nicotine using MβCD was investigated and compared with βCD to evaluate the preservation and skin permeation of nicotine. The M06-2X/6-31G(d,p) density functional theory calculations indicate a 1:1 host–guest molar ratio for the inclusion complex of nicotine with βCD and MβCD, and this was also validated by experimental studies using the TGA, DSC, XRD, and FTIR techniques. The preservation study of the nicotine/CDs inclusion complex compared to pure nicotine shows a stability improvement of nicotine after encapsulation by βCD and MβCD in the form of solid inclusion complexes. The remaining nicotine after 21 days is increased from 65.56% in pure nicotine to 89.32% and 76.22% in the nicotine/βCD and nicotine/MβCD inclusion complexes, respectively. This can be explained by the DFT calculations that nicotine forms considerably stronger binding to βCD than MβCD in the same orientation with lower complexation energy (ΔE). The skin permeation study, which is an important factor for transdermal patch application, shows that the amount of permeated nicotine depends on the stability of nicotine. Hence, the nicotine/βCD inclusion complex provides the highest permeated nicotine through pig skin as well. After 60 min, the amounts of nicotine permeated through pig skin from the nicotine/βCD and nicotine/MβCD inclusion complex gels are 14 and 10 times as much as the pure nicotine gel, respectively. In conclusion, the encapsulation technique with βCD and MβCD can be used to increase the shelf life of nicotine-containing products and the enhancement of skin permeability for further use in the pharmaceutical industry.

Author Contributions: Conceptualization, S.C., P.T. and L.L.; methodology, S.C., K.J., P.T. and L.L.; investigation, S.C., K.J. and L.L.; writing—original draft preparation, S.C. and K.J.; writing—review and editing, S.K., K.J., P.T. and L.L.; and supervision, P.T. and L.L. All authors have read and agreed to the published version of the manuscript.

Funding: Thammasat University Research Fund, Contract No. TUFT 068/2563.

Institutional Review Board Statement: Not applicable.

Informed Consent Statement: Not applicable.

Acknowledgments: The authors gratefully acknowledge the Center of Scientific Equipment for Advanced Research, Thammasat University (TUCSEAR) and Thailand Institute of Scientific and Technology Research (TISTR) for providing access to the analytical instruments.

Conflicts of Interest: The authors declare no conflict of interest.

References

1. Tayoub, G.; Sulaiman, H.; Alorfi, M. Determination of nicotine levels in the leaves of some Nicotiana tabacum varieties cultivated in Syria. *Herba Pol.* **2015**, *61*, 23–30. [CrossRef]
2. Benowitz, N.L. Pharmacology of nicotine: Addiction and therapeutics. *Annu. Rev. Pharmacol. Toxicol.* **1996**, *36*, 597–613. [CrossRef] [PubMed]
3. Balandrin, M.F.; Klocke, J.A.; Wurtele, E.S.; Bollinger, W.H. Natural plant chemicals: Sources of industrial and medicinal materials. *Science* **1985**, *228*, 1154–1160. [CrossRef] [PubMed]
4. Powledge, T.M. Nicotine as therapy. *PLoS Biol.* **2004**, *2*, e404. [CrossRef] [PubMed]
5. Newhouse, P.A.; Potter, A.; Kelton, M.; Corwin, J. Nicotinic treatment of Alzheimer's disease. *Biol. Psychiatry* **2001**, *49*, 268–278. [CrossRef]
6. Rusted, J.M.; Newhouse, P.A.; Levin, E.D. Nicotinic treatment for degenerative neuropsychiatric disorders such as Alzheimer's disease and Parkinson's disease. *Behav. Brain Res.* **2000**, *113*, 121–129. [CrossRef]
7. White, H.K.; Levin, E.D. Four-week nicotine skin patch treatment effects on cognitive performance in Alzheimer's disease. *Psychopharmacology* **1999**, *143*, 158–165. [CrossRef] [PubMed]
8. Hădărugă, D.I.; Hădărugă, N.G.; Butnaru, G.; Tatu, C.; Gruia, A. Bioactive microparticles (10): Thermal and oxidative stability of nicotine and its complex with β-cyclodextrin. *J. Incl. Phenom. Macrocycl. Chem.* **2010**, *68*, 155–164. [CrossRef]
9. Del Valle, E.M. Cyclodextrins and their uses: A review. *Process Biochem.* **2004**, *39*, 1033–1046. [CrossRef]
10. Pinho, E.; Grootveld, M.; Soares, G.; Henriques, M. Cyclodextrins as encapsulation agents for plant bioactive compounds. *Carbohydr. Polym.* **2014**, *101*, 121–135. [CrossRef] [PubMed]
11. Ezhilarasi, P.; Karthik, P.; Chhanwal, N.; Anandharamakrishnan, C. Nanoencapsulation techniques for food bioactive components: A review. *Food Bioproc. Technol.* **2013**, *6*, 628–647. [CrossRef]
12. Szente, L.; Szejtli, J. Highly soluble cyclodextrin derivatives: Chemistry, properties, and trends in development. *Adv. Drug Deliv. Rev.* **1999**, *36*, 17–28. [CrossRef]
13. Berglund, J.; Cedergren, L.; Andersson, S.B. Determination of the stability constant for the inclusion complex between β-cyclodextrin and nicotine using capillary electrophoresis. *Int. J. Pharm.* **1997**, *156*, 195–200. [CrossRef]
14. JS, P.; Kadam, D.; Marapur, S.; Kamalapur, M. Inclusion complex system; a novel technique to improve the solubility and bioavailability of poorly soluble drugs: A review. *Int. J. Pharm. Sci. Rev. Res.* **2010**, *2*, 29–34.
15. Jiang, Z.; Tang, G.; Zhang, Y.; Zhao, J. catena-Poly [[dibromidomercury (II)]-μ-3-(1-methylpyrrolidin-2-yl) pyridine-κ2N: N′]. *Acta Crystallogr. Sect. E Struct. Rep. Online* **2008**, *64*, m1319. [CrossRef] [PubMed]
16. Steiner, T.; Koellner, G. Crystalline. Beta.-cyclodextrin hydrate at various humidities: Fast, continuous, and reversible dehydration studied by X-ray diffraction. *J. Am. Chem. Soc.* **1994**, *116*, 5122–5128. [CrossRef]
17. Manunza, B.; Deiana, S.; Pintore, M.; Gessa, C. Structure and internal motion of solvated beta-cyclodextrine: A molecular dynamics study. *J. Mol. Struct. THEOCHEM* **1997**, *419*, 133–137. [CrossRef]
18. Biovia, D.S. *Discovery Studio Visualizer*; Dassault Systèmes: San Diego, CA, USA, 2017.
19. Frisch, M.J.; Trucks, G.W.; Schlegel, H.B.; Scuseria, G.E.; Robb, M.A.; Cheeseman, J.R.; Scalmani, G.; Barone, V.; Petersson, G.A.; Nakatsuji, H.; et al. *Gaussian 16 Rev. C.01*; Gaussian, Inc.: Wallingford, CT, USA, 2016.
20. Morris, G.M.; Huey, R.; Lindstrom, W.; Sanner, M.F.; Belew, R.K.; Goodsell, D.S.; Olson, A.J. AutoDock4 and AutoDockTools4: Automated docking with selective receptor flexibility. *J. Comput. Chem.* **2009**, *30*, 2785–2791. [CrossRef] [PubMed]
21. Sinlikhitkul, N.; Toochinda, P.; Lawtrakul, L.; Kuropakornpong, P.; Itharat, A. Encapsulation of plumbagin using cyclodextrins to enhance plumbagin stability: Computational simulation, preparation, characterization, and application. *J. Incl. Phenom. Macrocycl. Chem.* **2019**, *93*, 229–243. [CrossRef]
22. Cilurzo, F.; Minghetti, P.; Sinico, C. Newborn pig skin as model membrane in in vitro drug permeation studies: A technical note. *AAPS PharmSciTech* **2007**, *8*, 97–100. [CrossRef] [PubMed]

23. Sharma, A.; Jain, C.P.; Tanwar, Y.S. Preparation and characterization of solid dispersions of carvedilol with poloxamer 188. *J. Chil. Chem. Soc.* **2013**, *58*, 1553–1557. [CrossRef]
24. Cui, F.; Li, Y.; Zhou, S.; Jia, M.; Yang, X.; Yu, F.; Ye, S.; Hou, Z.; Xie, L. A comparative in vitro evaluation of self-assembled PTX-PLA and PTX-MPEG-PLA nanoparticles. *Nanoscale Res. Lett.* **2013**, *8*, 1–8. [CrossRef] [PubMed]